

# Superbubbles as the source of ${}^6\text{Li}$ , Be and B in the early Galaxy

E. Parizot and L. Drury

Dublin Institute for Advanced Studies, 5 Merrion Square, Dublin 2, Ireland (parizot, ld@cp.dias.ie)

Received 1 April 1999 / Accepted 31 May 1999

**Abstract.** We investigate the spallative production of the light elements, Li, Be and B (LiBeB), associated with the evolution of a superbubble (SB) blown by repeated supernovae (SNe) in an OB association. It is shown that if about ten percent of the SN energy can power the acceleration of particles from the material inside the SB, the observed abundances of LiBeB in halo stars, as a function of O, can be explained in a fully consistent way over several decades of metallicity. In this model, the energetic particles (EPs) reflect the SB material, which is a mixing of the ejecta of previous SNe and of the swept-up ISM gas evaporated off the shell. We investigated two different energy spectra for the EPs: the standard cosmic ray source spectrum, or ‘SNR spectrum’, and a specific ‘SB spectrum’,  $E^{-\alpha} \exp(-E/E_0)$ , where  $\alpha = 1-1.5$  and  $E_0$  is of order a few hundreds of MeV/n, as results from the SB acceleration mechanism of Bykov & Fleishman (1992). While the latter spectrum is more efficient in producing LiBeB, the SNR spectrum can be reconciled with the observational data if an imperfect mixing of the SN ejecta with the rest of the SB material and/or a selective acceleration is invoked (enhancing the C and O abundance amongst the EPs by a factor of  $\sim 6$ ). One of the main consequences of our model is that the observed linear growth of Be and B abundances as a function of Fe/H expresses a dilution line rather than a continuous, monotonic increase of the metallicity. We propose an observational test of this feature. We also show that the recent  ${}^6\text{Li}$  observations in halo stars fit equally well in the framework of the SB model. Finally, we conjecture the existence of two sets of low-metallicity stars, differing in their Be/Fe or B/O abundance ratios, resulting from a ‘bimodal’ LiBeB production in the Galaxy, namely from correlated (in SBs) or isolated SN explosions.

**Key words:** acceleration of particles – nuclear reactions, nucleosynthesis, abundances – ISM: cosmic rays – Galaxy: abundances

## 1. Introduction

It is generally accepted that all the elements in the universe have been produced (synthesized) in stars or stellar explosions, except the so-called primordial (H, He and part of the  ${}^7\text{Li}$ ), and light elements (Li, Be and B). The former class of nuclei is sat-

isfactorily accounted for by Big Bang nucleosynthesis models, while the latter is thought to be produced by non thermal processes in the interstellar medium (ISM). Indeed,  ${}^6\text{Li}$ , Be and B nuclei ( ${}^6\text{LiBeB}$ ) are actually destroyed rather than produced through the thermal nuclear processes in stellar interiors. The first, and most natural thesis concerning the origin of these light elements (Reeves et al. 1970, Meneguzzi et al. 1971) claimed that they were produced through spallation reactions of C and O nuclei induced by the interaction of the Galactic cosmic rays (mostly composed of protons and alpha particles, especially in the early, metal-poor Galaxy) with the ambient ISM. This process is referred to as the Galactic cosmic ray nucleosynthesis (GCRN). As the Galaxy evolves, the ISM gets richer and richer in C and O, making the spallative nucleosynthesis more and more efficient (one particular energetic proton has more chance to hit a C or O nucleus). As a consequence of the production rates being proportional to the ambient C and O abundance, the GCRN models predict an increase of the  ${}^6\text{LiBeB}$  abundance in the ISM, and thus in stars, proportional to the square of the metallicity, defined either as the O or Fe abundance.

However, the measurement of Be, B, and most recently  ${}^6\text{Li}$  abundances in very metal-poor stars of the Galactic halo has considerably changed this picture (see e.g. Vangioni-Flam et al., 1998, for a review). Two important problems have arisen. The first one is qualitative: the increase of Be and B is found to be proportional to the Fe abundance (instead of its square) for stars of metallicity ranging from  $10^{-3}$  to  $10^{-1}$  times the solar metallicity. The second problem is quantitative: the amount of Be and B nuclei effectively observed in halo stars requires an extremely large number of spallation reactions, as compared to what can be expected from the standard GCRN scenario. This, in turn, implies that an enormous amount of energy has been imparted to the cosmic rays in the early Galaxy.

The most natural answer to both of these problems (qualitative and quantitative) is to assume that the energetic particles (EPs) inducing the spallation reactions are not representative of the ambient ISM at the time of their acceleration, as in the case of GCRN, but rather show a much richer abundance in C and O, so that the  ${}^6\text{LiBeB}$  nucleosynthesis is mainly due to energetic C and O nuclei being spalled in flight on H and He nuclei at rest in the ISM (so-called *inverse spallation*), rather than the opposite, i.e. energetic H and He interacting with C and O nuclei at rest (so-called *direct spallation*). In this way, the  ${}^6\text{LiBeB}$  spallative

production rate in the Galaxy depends only on the power, composition and energy spectrum of the EPs, not on the composition of the ambient ISM. It is therefore directly proportional to the EP acceleration rate in the Galaxy, and thus presumably to the supernova explosion rate. As a consequence, the abundance of  ${}^6\text{LiBeB}$  increases proportionally to that of C and O, in agreement with the observations. Moreover, since the EPs are C and O rich, the efficiency of the nucleosynthetic process is much higher than in the case of GCRN, where a lot of energy is imparted to (and lost in) protons and alpha particles which never hit any C or O nucleus in the ISM to produce light elements.

This idea of a process dominated by inverse spallation reactions has been discussed in a number of phenomenological papers (e.g. Cassé et al. 1995, Ramaty et al. 1996, 1997, Vangioni-Flam et al. 1998). However, while this solution framework clearly improves the situation, some important questions still need to be answered: what is the composition of the EPs responsible for the production of the  ${}^6\text{LiBeB}$  nuclei observed in halo stars? What is the EP energy spectrum? What is their source of energy? What is the acceleration mechanism? How efficient is it? Where does the acceleration take place? Where do the spallation reactions take place? All these questions are linked together in more or less complex a way, as the energy requirement of the  ${}^6\text{LiBeB}$  production depends on the composition and spectrum of the EPs, both of which depend in turn on the acceleration site and mechanism.

In a pair of recent papers (Parizot & Drury 1999a,b), we have investigated in detail two light elements production mechanisms associated with the explosion of a supernova in the ISM, and calculated the total amount of Be they produce. While both of these processes are *primary* and therefore reproduce the observed linear growth of  ${}^6\text{LiBeB}$  abundances as a function of metallicity, we showed that they fail to solve the quantitative part of the problem, and must therefore be abandoned. Analyzing the reasons for this failure, we pointed out one possible alternative scenario, based on the acceleration of enriched material within superbubbles. Such a model, focusing on the collective effect of many supernovae occurring repeatedly in OB associations, rather than on individual supernovae, is now investigated in detail in this paper.

## 2. Description of the model

### 2.1. Overview

We are interested in the total production of Li, Be and B associated with the evolution of a typical superbubble (SB) generated by the supernova activity of an OB association in the interstellar medium. The basic idea is the following: when several SN explosions occur locally both in space and time, a superbubble forms and grows, surrounded by a shell of swept-up ISM gas. Its interior is filled with hot ( $T > 10^6$  K), tenuous ( $n \lesssim 10^{-2}$ ) gas, made of i) the ejecta of previous supernovae and possible winds of massive stars and ii) the interstellar material evaporated off the shell or embedded clouds. When a new supernova explodes within an already formed superbubble, part of its energy powers some acceleration process (usual SN shock acceleration or

any other specific process) and goes into EPs which then induce spallation reactions by which a certain amount of LiBeB is produced. The specificity of the SB model is twofold: i) since the interior of the SB receives the ejecta of previous SNe, the composition of the EPs is naturally enriched in C and O, even in the absence of selective acceleration, which makes the LiBeB production particularly efficient and ii) the energy spectrum of the EPs may be different from the usual CR source spectrum, as a result of a possibly different acceleration mechanism due to the specific physical conditions prevailing inside the SB (Bykov & Fleishman, 1992; Bykov, 1995,1999).

An other specific feature of our SB model is that it implies a discontinuous increase of the LiBeB abundance in the ISM. Unlike the ‘ISM models’ where both metals and light elements build up continuously as the stars process the primordial Galactic gas in the ISM and progressively increase its metallicity, the SB model provides a locally strong increase of the metallicity and the LiBeB abundance, resulting from the accumulation of the ejecta of many massive stars in a small region of space (the SB), on a relatively short time scale (a few tens of Myr). Anticipating the main result of this paper, we emphasize that a typical SB developing in the very early Galaxy (with a mean ISM metallicity  $Z = 10^{-4}Z_{\odot}$ ) provides after, say, 30 Myr, about  $8 \cdot 10^4 M_{\odot}$  of material with metallicity  $Z = 10^{-1}Z_{\odot}$  and the correct (i.e. observed) LiBeB abundances relative to this metallicity. When the SB then breaks up, these  $\sim 8 \cdot 10^4 M_{\odot}$  of high metallicity material mix with the ambient ISM, whose metallicity is three orders of magnitude lower in our canonical example. Depending on the mixing or dilution efficiency, the SB gives rise to concentrations of matter with various metallicities, extending from  $Z = 10^{-1}Z_{\odot}$  (virtually no dilution) to  $Z = 10^{-4}Z_{\odot}$  (dilution of the SB material by a large amount of ISM gas). The next generation of stars formed from the collapse of this variously enriched gas will thus show very different metallicities, but always the same abundance ratios (such as Be/O, or B/Fe), namely those of the parent SB itself. This model therefore predicts constant abundance ratios (including those involving  ${}^6\text{LiBeB}$ ) over several decades of metallicity, in conformity with the observations. But the linear increase of, say, the Be abundance as a function of Fe/H, now has a very different origin: it is essentially a *dilution line*, not a ‘constant growth line’, or ‘accumulation line’.

In addition, this also implies that the relation between the age and metallicity of the metal-poor stars is no longer monotonic and one-to-one. Two stars formed at the same time from the gas processed in a given SB can indeed show very different metallicities, depending on the dilution of this gas with the ambient ISM before the gravitational collapse. This is in contrast with the Galactic chemical evolution models where a steady, continuous enrichment of the interstellar gas is assumed. An observational test of this important feature is suggested in Sect. 4.

### 2.2. The superbubble model

The detailed structure and evolution law of a given superbubble obviously depends on the local density profile as well as on the

history of the SN explosions, determined by the particular stellar content and stellar formation history of the OB association. However, since we are only interested in the mean LiBeB yield per supernova or per superbubble, we shall make some general simplifying assumptions to calculate the output to be expected from a ‘typical superbubble’.

Following previous work on the evolution of superbubbles in the ISM (e.g. Mac Low & McCray 1988), we shall assume a continuous power supply from SN explosions regularly spread in time in a localized OB association, within a homogeneous ISM. The resulting SB is therefore spherically symmetric and can be treated by the standard self-similar model of Weaver et al. (1977) for a pressure-driven wind bubble. The expressions for the SB radius, mass, internal mean density and temperature then read:

$$R_{\text{SB}}(t) = (66 \text{ pc}) L_{38}^{1/5} n_0^{-1/5} t_{\text{Myr}}^{3/5} \quad (1)$$

$$M_{\text{SB}}(t) = (1600 M_{\odot}) L_{38}^{27/35} n_0^{-2/35} t_{\text{Myr}}^{41/35} \kappa_0^{2/7} \quad (2)$$

$$n_{\text{SB}}(t) = (1.6 \cdot 10^{-2} \text{ cm}^{-3}) L_{38}^{6/35} n_0^{19/35} t_{\text{Myr}}^{-22/35} \kappa_0^{2/7} \quad (3)$$

$$T_{\text{SB}}(t) = (5.3 \cdot 10^6 \text{ K}) L_{38}^{8/35} n_0^{2/35} t_{\text{Myr}}^{-6/35} \kappa_0^{-2/7} \quad (4)$$

where  $L_{38}$  is the mechanical luminosity of the OB association (assumed constant) in units of  $10^{38} \text{ erg s}^{-1}$ ,  $n_0$  is the ISM number density in  $\text{cm}^{-3}$ , and  $t_{\text{Myr}}$  is the SB age in Myr. The mass of the SB is mainly due to conductive evaporation from the shell. Following Shull & Saken (1995), we have multiplied the classical conductivity by a dimensionless scaling factor  $\kappa_0 \leq 1$  to account for possible magnetic suppression. As can be seen in the above equations, the dependence of  $M_{\text{SB}}$  and  $n_{\text{SB}}$  on  $\kappa_0$  is rather weak, so that the magnetic suppression would have to be very strong ( $\kappa_0 \ll 1$ ) to produce a large diminution of the SB mass and density, at a given time.

Higdon et al. (1998) have distinguished between magnetic and non-magnetic models in a different way: referring to Tomisaka (1992)’s numerical model of magnetized SBs, they assumed that the mass injected into the SB averages about  $45 M_{\odot}$  per supernova. This implies a much lower SB mass, so that the enriched ejecta of the SNe are less diluted and the composition of the SB material to be accelerated is correspondingly much richer in C and O. However, this model does not seem very realistic, considering the extremely low SB density which it implies:  $n_{\text{SB}} \sim 2 \cdot 10^{-4} \text{ cm}^{-3}$  for  $t_{\text{SB}} = 50 \text{ Myr}$  (Higdon et al., 1998), to be compared with typical values inferred from the observations of order  $\gtrsim 10^{-2} \text{ cm}^{-3}$  (e.g. Brown et al., 1995; Bomans et al., 1997; Walter et al., 1998), in better agreement with Eq. (3). Moreover, the value of  $45 M_{\odot}$  used by Tomisaka is, on his own admission, arbitrary, and taken essentially to ensure the numerical stability of his code. Therefore, we shall not use this low-mass model here, and hold on to the ‘canonical’ SB model described by Eqs. (1)–(3).

The typical parameters which we use are the following:  $n_0 = 1 \text{ cm}^{-3}$ ,  $\kappa_0 = 1$ , and  $L_{38} = 1$ , which corresponds to one SN explosion every  $\sim 3 \cdot 10^5 \text{ yr}$  (for an explosion energy

$E_{\text{SN}} = 10^{51} \text{ erg}$ ). Assuming a lifetime of 30 Myr for the SB thus amounts to saying that the OB association provides a total of 100 SNe. However, we also investigate less active SBs, with mechanical luminosities  $L_{38} = 0.1$ , and poorer OB associations with only a few tens of SNe.

### 2.3. The production of light elements in superbubbles

To calculate the LiBeB production associated with the SB evolution, we apply the time dependent model described in Parizot & Lehoucq (1999). To do so, we first determine the so-called injection function,  $Q(E, t)$ , which gives the power per unit energy imparted to the EPs, as well as their energy spectrum and composition as a function of time (for more details, see Parizot & Drury, 1999b, where the model is applied in much the same way to the spallative nucleosynthesis in supernova remnants). Then we let the EPs interact with the surrounding medium, in which they suffer energy losses and nuclear reactions, some of which lead to LiBeB production. We thus deduce the production rates as a function of time, and integrate them to obtain the total yields in the light elements:  $\mathcal{N}_{\text{Li}}$ ,  $\mathcal{N}_{\text{Be}}$  and  $\mathcal{N}_{\text{B}}$ .

We assume that the power imparted to the EPs is, at any time, a fraction  $\theta$  of the total mechanical power supplied by the OB association. In the early Galaxy, the contribution of the winds of massive stars is thought to be very small, because of the low stellar metallicity, so the available energy is mainly due to the SN explosions. In conformity with standard shock acceleration models, we assume  $\theta = 0.1$ , but the results can be scaled straightforwardly to any other value. As for the EP energy spectrum, we investigated two different forms: i) a standard shock acceleration spectrum, i.e.  $Q(p) \propto p^{-4}$ , thought to be also the CR source spectrum, and called here the ‘SNR spectrum’ to emphasize that it originates at an isolated supernova remnant, and ii) a ‘SB spectrum’,  $Q(E) \propto E^{-\alpha} \exp(-E/E_0)$ , where  $\alpha = 1$  or 1.5, and  $E_0$  is a cut-off energy of typically a few hundreds of MeV/n. This spectrum is taken as an approximate of the time-dependent source spectrum derived from an acceleration model relevant to the specific physical conditions prevailing within a SB (Bykov & Fleishman, 1992; Bykov, 1995, 1999).

While the SB evolves, more and more particles get accelerated and contribute to the LiBeB production rates. We assume that the EPs are confined within the SB during its whole lifetime, as a consequence of the magnetic waves and strong magnetic turbulence. This implies that they interact with the enriched SB material. However, this assumption is of little influence on the total LiBeB yields, because it is found that the spallative nucleosynthesis is dominated by inverse spallation processes, which are essentially independent of the target composition. Moreover, since the SB density is very low, most of the EPs have not yet been spalled and still have a supernuclear energy at the end of the SB lifetime ( $t = \tau_{\text{SB}}$ ). They then diffuse away in the surrounding medium, interact with the ISM gas in the dense shell or stay confined for a while within the dislocating SB. Again, their genuine fate is not crucial to our calculations, since the total LiBeB production (i.e. integrated over time) is independent of both the target composition (as long as it is much poorer

in C and O than the EPs are) and density. For simplicity, we assume here that the target composition after  $\tau_{\text{SB}}$  is the ISM composition, and its density is  $0.1 \text{ cm}^{-3}$ . This rather low value weakens the discontinuity of the production rates (see Fig. 5) and ensures a smooth numerical behavior. However, when we want to show some specific behaviors such as the dependence of the production rates on the ambient density or the EP spectrum (Figs. 6 and 7), we assume that the target density after  $\tau_{\text{SB}}$  is equal to  $n_{\text{SB}}(\tau_{\text{SB}})$ , which provides continuous curves. On the other hand, it implies artificially long timescales, even longer than the age of the Galaxy. In reality, once the SB dislocates and/or the EPs leave the SB interior, the mean density of the medium in which they propagate increases rapidly, making the spallation timescales much shorter (by the same factor as the density ratio). Most probably, the main target for the EPs is the shell surrounding the SB, whose density is higher than the ambient ISM.

#### 2.4. The EP composition

Most important also is the composition of the EPs. Whatever the acceleration mechanism at work within the SB, the particles to be accelerated are those who stand in the hot bubble where the energy is released. If the acceleration mechanism is not selective (i.e. the acceleration efficiency is independent of the nuclear species), the EP composition is thus nothing but the composition of the material inside the SB, which is a mixing of the SN ejecta accumulated at time  $t$  and the ISM material evaporated from the shell. Higdon et al. (1998) have argued that SN explosions occur mainly in the core of superbubbles where the metallicity is dominated by the SN ejecta. However, this does not mean that there is no dilution at all. In the very early Galaxy, the ISM contains no metals, so the metallicity of the SB interior is certainly dominated by the SN ejecta, wherever the new explosion occurs and the particle acceleration takes place. However, the composition of the EPs still depends on the mixing of the ejecta with the ISM material evaporated from the shell. Moreover, some metal-poor material may be evaporated from high density clouds embedded in the SB (e.g. Cioffi & Shull, 1991; Zanin & Weinberger, 1997), close enough to the core to be accelerated directly by the SN shock.

To evaluate the degree of gas mixing, we assume that it occurs on a timescale  $\tau_{\text{mix}} = R_{\text{SB}}/V_{\text{mix}}$ , where  $V_{\text{mix}}$  is a ‘turbulent velocity’ of the order of the sound speed,  $c_s$ , and compare  $\tau_{\text{mix}}$  with the age of the SB,  $t$ . Calculating  $c_s$  from the SB temperature, Eq. (4), we obtain:

$$\tau_{\text{mix}} \simeq (0.67 \text{ Myr}) \left( \frac{L_{38} t_{\text{Myr}}}{n_0} \right)^{1/5}. \quad (5)$$

The condition for the mixing time to be smaller than the SB age, i.e.  $\tau_{\text{mix}} < t$ , then reads:

$$t > (5 \cdot 10^5 \text{ yr}) \sqrt{\frac{L_{38}}{n_0}}. \quad (6)$$

We thus find that the gas evaporated from the SB should have had enough time to mix with the SN ejecta as soon as

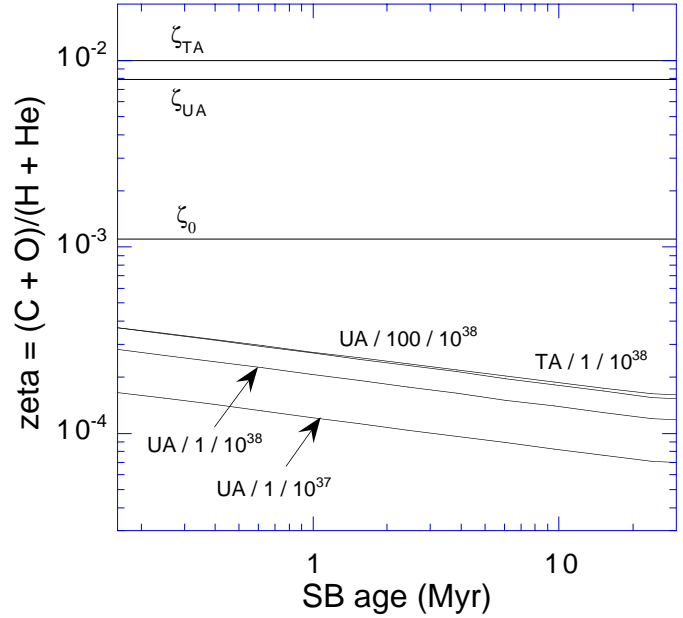


**Fig. 1.** Evolution of the reduced metallicity,  $\zeta$ , over the superbubble lifetime (here, 30 Myr). The labels indicate, respectively, the SN model used (from WW95), the ambient density (in  $\text{cm}^{-3}$ ) and the mechanical power (in  $\text{erg s}^{-1}$ ). Also shown are the solar reduced metallicity ( $\zeta_0$ ), and the reduced metallicity corresponding to the pure ejecta for models UA and TA of WW95 (the compositions have been averaged over an IMF of index 2.35).

$t \gtrsim 5 \cdot 10^5 \text{ yr}$ , i.e. after the explosion of the first or second SN. To take this result into account, we assume that the EP composition at any time reflects that of the accumulated SN ejecta diluted by and perfectly well mixed with the ISM gas evaporated at that time. Note that this is a conservative assumption, as imperfect mixing and/or selective acceleration could raise the C and O abundance amongst the EPs, and thus increase the LiBeB yields.

Fig. 1 shows the evolution of the EP composition as a function of time, for different SN models, ambient densities and SB mechanical powers. We use the explosion models of Woosley & Weaver (1995, hereafter WW95) for OB stars of initial metallicity  $Z = 10^{-4} Z_{\odot}$  (models U), and  $Z = 10^{-2} Z_{\odot}$  (models T), averaging all the yields over an initial mass function (IMF) of index  $x$ . We found that the results do not change significantly for any reasonable value of  $x$ , so we only show the results obtained with the Salpeter index  $x = 2.35$ . The efficiency of LiBeB production and the elemental and isotopic ratios obtained actually depend mostly on the ratio of the number of C and O nuclei to that of H and He. As a consequence, we can conveniently specify the composition of the EPs by using one single parameter,  $\zeta$ , which we call the *reduced metallicity* and define as:

$$\zeta = \frac{{}^{12}\text{C} + {}^{16}\text{O}}{{}^1\text{H} + {}^4\text{He}}, \quad (7)$$

where  ${}^{12}\text{C}$ , e.g., is the number abundance of the  ${}^{12}\text{C}$  nuclei amongst the EPs. By way of comparison, the solar reduced

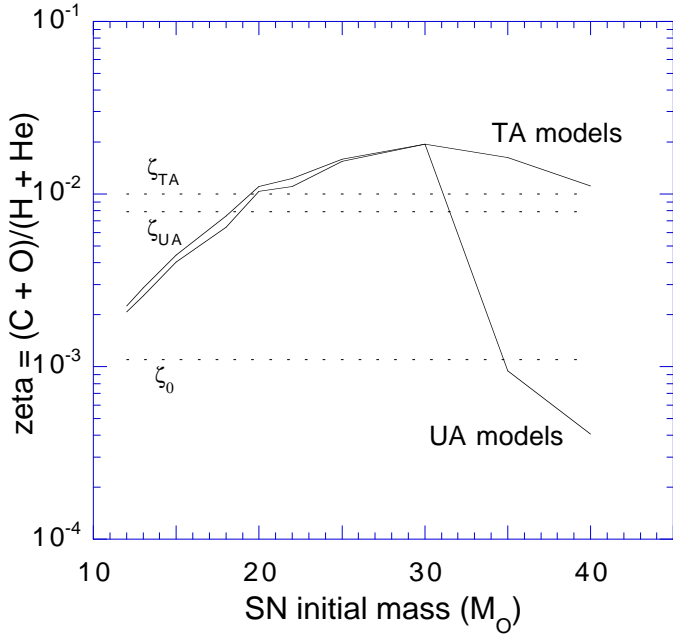


**Fig. 2.** Reduced metallicity,  $\zeta$ , for different SN explosion models (from WW95), as a function of the initial mass of the progenitor. Also shown are the solar reduced metallicity ( $\zeta_{\odot}$ ), and the mean reduced metallicity for models UA and TA.

metallicity is (with the abundances given by Anders & Grevesse, 1989):

$$\zeta_{\odot} = 1.1 \cdot 10^{-3}. \quad (8)$$

As can be seen from Fig. 1,  $\zeta_{EP}$  is about 30 to 100 times lower than the reduced metallicity of the pure ejecta, which results from the dilution of the EPs with the very metal-poor ISM gas ( $Z = 10^{-4}Z_{\odot}$  for models U, and  $Z = 10^{-2}Z_{\odot}$  for models T). Moreover, the reduced metallicity of the EPs (at injection) decreases as  $t^{-6/35}$ , because the total SB mass increases as  $t^{41/35}$  (see Eq. (2)), while the number of SNe and hence the mass of the ejecta is merely proportional to time (constant SN power). On the other hand, a higher ambient density and a higher explosion rate (SB mechanical power) both imply a smaller dilution, i.e. EPs richer in C and O and thus higher spallation yields.

Of course, the above assumption that the SN explosion rate is constant is certainly wrong, but as we discuss below (Sect. 4), this affects the injection rate of metals and the mechanical power in the same way. Reformulating the problem in terms of an ‘effective time’ so that the corresponding effective SN rate is constant would then lead to very similar results. However, a more subtle effect may lead to departures from our function  $zeta(t)$  (shown in Fig. 1): it is the fact that very massive stars eject more material and have a shorter life than less massive SN progenitors. As a consequence, at early times of SB evolution, the mass of metals ejected per unit power released should be higher than at the later times. Clearly, if the first star to explode has a  $36 M_{\odot}$  progenitor, the induced reduced metallicity shall be two times larger than the value calculated above with our average model, which assumes that all the SNe have the same mass (i.e. the

average SN mass over the IMF, namely  $18 M_{\odot}$ ) and the same ejecta (the mean ejecta of all SN progenitors). This increase in the early value of  $\zeta_{EP}$  will of course increase the LiBeB production. However, it shall be compensated by a corresponding decrease at later times, when lower mass SNe explode, with smaller mass of metals ejected per unit of power released. On the average, we don’t expect that the total integrated yields of LiBeB should be very different from those calculated below, with the ‘average SN’ model (although the non stationarity of the model prevents a perfect cancellation of the effects).

An other effect which could slightly change the results of our average model is the fact that the reduced metallicity of the ejecta actually depends on the mass of the progenitor. This is shown in Fig. 2, for both UA and TA models. As can be seen,  $\zeta_{ej}$  peaks for progenitors of  $\sim 30 M_{\odot}$ , where it is about two times higher than the average value. Therefore, as above, if the first SN to explode is a  $30 M_{\odot}$  star, we should expect values of  $\zeta_{EP}$  about two times higher than our average value. Again, however, this should not affect the total LiBeB yields too much, as the effect will be compensated by lower  $\zeta_{EP}$  at later times. However, it is worth noting that the history of the LiBeB production can be different for different explosion histories in the OB association (high masses first or low masses first), and contrary to LiBeB nucleosynthesis, this would have a very significant influence on the gamma-ray line emission rates associated with the EP interactions (to be addressed in future works).

## 2.5. Comparison with the observations

To compare the results of our SB model with the observations, we need to calculate the LiBeB as well as the Fe and O yields of the SB at the end of its life. The former are the output of our time-dependent calculations, while the latter are taken from the SN explosion models of WW95, averaged over the IMF, and multiplied by the number of SNe in the OB association. A successful model will then be a model which reproduces all the observed chemical abundance ratios. The easiest way to check this is to compute the isotopic and elemental ratios of the light elements on the one hand, and the Be/O and Be/Fe ratios on the other hand.

The question of the LiBeB abundance ratios has been studied in detail in previous works (e.g. Ramaty et al. 1997, Vangioni-Flam et al. 1998, Vangioni-Flam & Cassé 1999), so we focus here on the Be/O and Be/Fe ratios, which are the most problematic. We only recall that the yields of Li, Be and B must satisfy  $\mathcal{N}_{\text{Li}}/\mathcal{N}_{\text{Be}} < 100$ , not to overproduce Li and ‘break the Spite plateau’, and  $10 \lesssim \mathcal{N}_{\text{B}}/\mathcal{N}_{\text{Be}} \lesssim 30$ . Both of these constraints are satisfied by our SB model, although the values which we obtain for the B/Be abundance ratio lay at the lower end of the above interval, i.e.  $\text{B/Be} \gtrsim 10$ . However, it must be kept in mind that part of the Boron is believed to be produced by neutrino-spallation, during the SN explosions themselves. This is indeed the only known way to get a  ${}^{11}\text{B}/{}^{10}\text{B}$  isotopic ratio close to the meteoritic value of  $\sim 4$ , unless invoking a component of cosmic-rays with a very low-energy cut-off, which raises strong problems relating to the energetics (Ramaty et al. 1997). This means that the

genuine B/Be production ratio in the SB, *including the Boron produced by neutrino-spallation*, is always larger than the B/Be ratio derived from nuclear spallation only, which we calculate here. The SB value of, say,  $B/Be = 11$ , corresponding to a nuclear spallation isotopic ratio  ${}^{11}\text{B}/{}^{10}\text{B} \sim 2.2$ , implies a value of  $B/Be \gtrsim 17$  once scaled to  ${}^{11}\text{B}/{}^{10}\text{B} \gtrsim 4$ , which is thus in very good agreement with the observations. However, this agreement is not specific to the SB model, as most of the spallation models, whatever the EP composition and energy spectrum, would lead to essentially identical elemental and isotopic ratios. As a consequence, we shall pay more attention to the Be production as compared to O and Fe in the following, because this represents the most conclusive argument in favour of the SB model.

To have done with the LiBeB abundance ratios, we note that recent observational work also provided the first measurements of the  ${}^6\text{Li}$  isotope in two halo stars of metallicity  $Z \simeq 10^{-2.3}Z_{\odot}$  (Hobbs & Thorburn, 1994, 1997; Smith et al., 1998; Cayrel et al., 1999). The deduced  ${}^6\text{Li}/{}^9\text{Be}$  ratio in these stars is found to lay between 20 and 80 (although Be has not been measured directly in these particular stars), in contrast with the solar value of  $\sim 6$ .

Concerning the Be/Fe ratio, the observations show that it is approximately constant for stars of metallicity up to  $10^{-1}$  solar, and equal to  $\sim 1.6 \cdot 10^{-6}$  (e.g. Ramaty et al. 1997). This is the value which the SNR model failed to obtain (Parizot & Drury, 1999a,b), and the most constraining of all the observational requirements, in the present state of knowledge. Assuming an average Fe yield of  $0.11 M_{\odot}$  per SN, this requires a production of  $\sim 3.8 \cdot 10^{48}$  Be nuclei per SN. As for the Be/O ratio, the situation is less clear from the observational point of view, because there are no data at metallicities below  $10^{-2}Z_{\odot}$ . However, since the SB model predicts a constant Be/O ratio at low metallicity, we assume that this is actually the case, and derive a value of  $\sim 7.5 \cdot 10^{-5}$  from the available observational data (e.g. Fields & Olive, 1999).

Interestingly enough, the above Be/Fe and Be/O ratios are not mutually compatible, considering the Fe and O yields given by the SN models of WW95. This is due to the failure of these models to reproduce consistently the O and Fe evolution in halo stars, as for instance the observed increase of the O/Fe ratio towards the lowest metallicities (Israeli et al. 1998, Boesgaard et al. 1998), although a different mixing time of freshly synthesized Fe and O nuclei with the ISM gas may solve this problem (Ramaty & Lingenfelter, 1999). As far as the LiBeB production is concerned, however, the most relevant ratio to be compared with the observations is Be/O, as Oxygen is the main progenitor of Be, while the genuine Fe production in SNe has no influence at all on the Be yield of the SB. A simple solution to the problem might thus simply be that the SN models produce too much Fe at low metallicity, due possibly to a wrong determination of the mass cut-off (see Parizot & Drury, 1999c, for a discussion of this issue).

### 3. Results, analysis and discussion

#### 3.1. General results from steady-state calculations

Before we present the results of the SB model, it is worthwhile showing some general results obtained with steady-state calculations, for different EP spectra and compositions, as a function of the target metallicity. As already mentioned, H, He, C and O are the only relevant elements, so we use the reduced metallicity  $\zeta$  defined above instead of the usual  $Z$ .

In Fig. 3, we plot the Be production efficiency, defined as the number of Be nuclei synthesized per erg injected in the form of EPs, for different spectra, namely the cosmic-ray source spectrum and the ‘SB spectrum’ defined above, with spectral index  $\alpha = 1.5$  or  $\alpha = 1$ . In the latter case, two different cut-off energies have been used, as indicated on the plots. Finally, for each spectrum, we calculated the Be production efficiency for eleven values of the EP reduced metallicity, ranging from  $10^{-7}$  to  $10^3$  (recalling that  $\zeta_{\odot} = 1.1 \cdot 10^{-3}$ ). These curves enable one to quickly evaluate the Be production for any source and target composition, as well as for the most commonly used EP spectra. Their qualitative analysis is straightforward, and independent of the EP spectrum.

In the upper-left part of the figures, the Be production efficiency is an horizontal line for any given  $\zeta_{\text{EP}}$ , which indicates that the inverse spallation reactions dominate. As expected in this case, the production efficiency is independent of the target metallicity, whence the horizontal lines. Of course, this regime dominated by inverse spallations ends up at lower target metallicities for lower  $\zeta_{\text{EP}}$ , as can be seen on Fig. 3. Clearly visible on the figures is also the straight line with slope 1 where all the curves converge. This line corresponds to a Be production dominated by direct spallation reactions. This roughly amounts to say that the target metallicity is higher than the EP metallicity, so that the production efficiency is virtually independent of the EP composition. The reactions producing Be are of the type  $p, \alpha + \text{C, O}$ , and the production efficiency is just proportional to the target metallicity. In the upper-left part of the figures, where inverse spallation dominates, the opposite holds: the production efficiency is proportional to the EP (reduced) metallicity, except for very high  $\zeta$ , namely  $\zeta \gtrsim 0.1 \simeq 100 \zeta_{\odot}$ , where the process saturates. The corresponding value is thus the highest production efficiency which one can get with the particular spectrum considered. Increasing the target metallicity then brings all the curves together towards one particular point where the production efficiency is the same, whatever the EP composition. This ‘meeting point’ is seen to correspond to a target metallicity between 60 and 200 times solar. Above this point, the Be production efficiency is actually higher for lower EP metallicities. This results from the fact that in a very rich target, energetic H and He nuclei are more efficient than C and O, because at a given energy per nucleon, they carry much less energy.

This behavior of the production efficiency is exactly the same for B, although with values about 11 times higher (i.e.  $B/Be \sim 11$ ). We therefore do not show these curves here.

As for Li, we show on Fig. 4 the evolution of the  ${}^6\text{Li}/{}^9\text{Be}$  ratio under the same conditions as above. To understand the

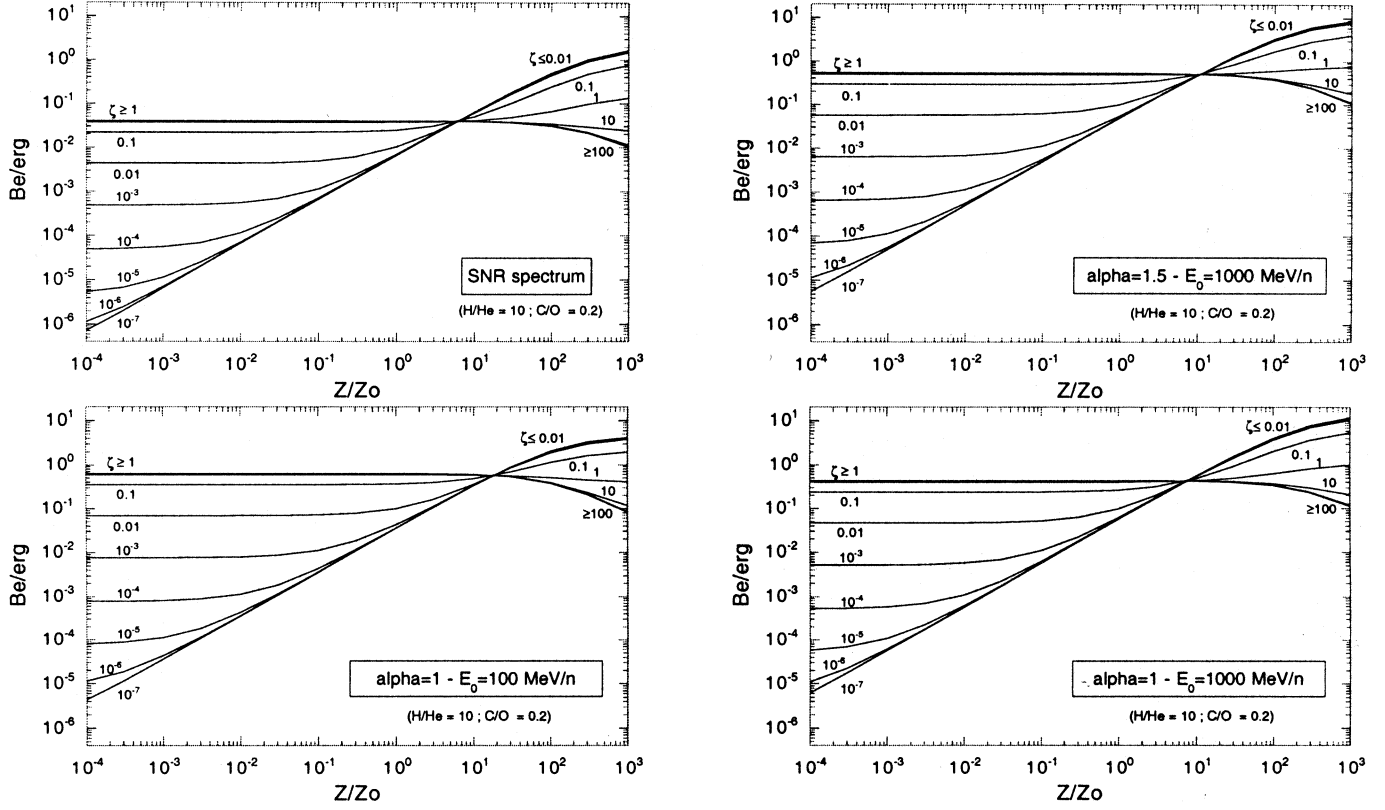


**Fig. 3.** Be production efficiency by spallation, in numbers of Be nuclei produced per erg of EPs injected in the ISM, for different energy spectra and EP compositions (as indicated on the figures), as a function of the ISM (target) metallicity, expressed in units of the solar metallicity. The labels refer to the reduced metallicity of the EPs,  $\zeta$ , defined in the text.

curves, one only needs to know that  ${}^6\text{Li}$  can be produced either by fusion reactions ( $\alpha + \alpha$ ) or by spallation reaction implying C, N or O nuclei, while  ${}^9\text{Be}$  can only be obtained by the latter processes. As a consequence, the  ${}^6\text{Li}/{}^9\text{Be}$  production ratio reflects the  $\text{He}/(\text{C} + \text{O})$  ratio either in the EPs or in the target. Two main regimes can be observed on Fig. 4, depending on whether fusion or spallation reactions dominate the  ${}^6\text{Li}$  production. For high enough EP metallicities ( $\zeta_{\text{EP}} \gtrsim 0.1$ ), spallation dominates, so that both  ${}^6\text{Li}$  and  ${}^9\text{Be}$  are produced in the same way. Their production ratio is thus essentially constant, determined by the ratio of the cross-sections (averaged over the spectrum). For lower EP metallicities, however, the  ${}^6\text{Li}/{}^9\text{Be}$  production ratio is proportional to the fusion/spallation production ratio of Li, or to the  $\text{He}/(\text{C} + \text{O})$  ratio, that is practically to  $\zeta_{\text{EP}}^{-1}$ , as seen on Fig. 4. Finally, the same behavior as for Be relative to the target metallicity can still be observed: at low  $Z$ , the  ${}^6\text{Li}/{}^9\text{Be}$  production ratio is independent of  $Z$ , because the inverse spallation reactions dominate, while when  $\zeta_{\text{target}} \gtrsim \zeta_{\text{EP}}$ ,  ${}^6\text{Li}/{}^9\text{Be}$  is inversely proportional to  $\zeta_{\text{target}}$ , because the direct spallation dominates (i.e. the  ${}^6\text{Li}$  production efficiency is constant while  ${}^9\text{Be}$ 's is proportional to  $\zeta_{\text{target}}$ ).

Coming now to the quantitative point of view, it turns out that Figs. 3 and 4 jointly provide important clues towards a solution of the  ${}^6\text{LiBeB}$  evolution problem in the Galaxy. As mentioned earlier, the observationally required Be production per SN is of order  $4 \cdot 10^{48}$ , if comparison is made with Fe, or  $\sim 6 \cdot 10^{47}$ ,

if comparison is made with O (assuming the averaged Oxygen yield of  $1.1 M_{\odot}$  per SN, derived from the models of WW95). If the mean SN explosion energy of  $10^{51}$  erg and the acceleration efficiency is 10%, this implies a Be production efficiency of  $\sim 4 \cdot 10^{-2}$  Be/erg (for comparison with Fe), or  $\sim 6 \cdot 10^{-3}$  Be/erg (for comparison with O), the latter being more reliable, as discussed above. Reporting to Fig. 3, it is easy to determine the EP reduced metallicity which is needed to get such an efficiency. Since we are interested in low-metallicity targets (early Galaxy), the correspondence between the Be production efficiency and  $\zeta_{\text{EP}}$  is one to one, once a spectrum is given. For a cosmic-ray source spectrum (Fig. 3a), an efficiency of  $6 \cdot 10^{-3}$  Be/erg requires an EP reduced metallicity about 20 times the solar value. This seems quite hard to achieve, even in the SB model, since Fig. 1 shows values between 50 and 200 times lower. On the other hand, a SB spectrum with a relatively low-energy cut-off can achieve the required Be production efficiency with values of  $\zeta_{\text{EP}}$  as low as a few  $10^{-4}$ , i.e. close to the values obtained naturally within the framework of our SB model.

Further referring to Fig. 4, it is quite interesting to see that our SB values for  $\zeta_{\text{EP}}$  of a few  $10^{-4}$  also predict a  ${}^6\text{Li}/{}^9\text{Be}$  production ratio decreasing from a few tens in low-metallicity targets to about 6 around solar metallicity. This is exactly the observed behavior, although more data on the  ${}^6\text{Li}$  abundance in low-metallicity stars are still needed to draw a definite conclusion. We should also mention that Vangioni-Flam et al. (1999)

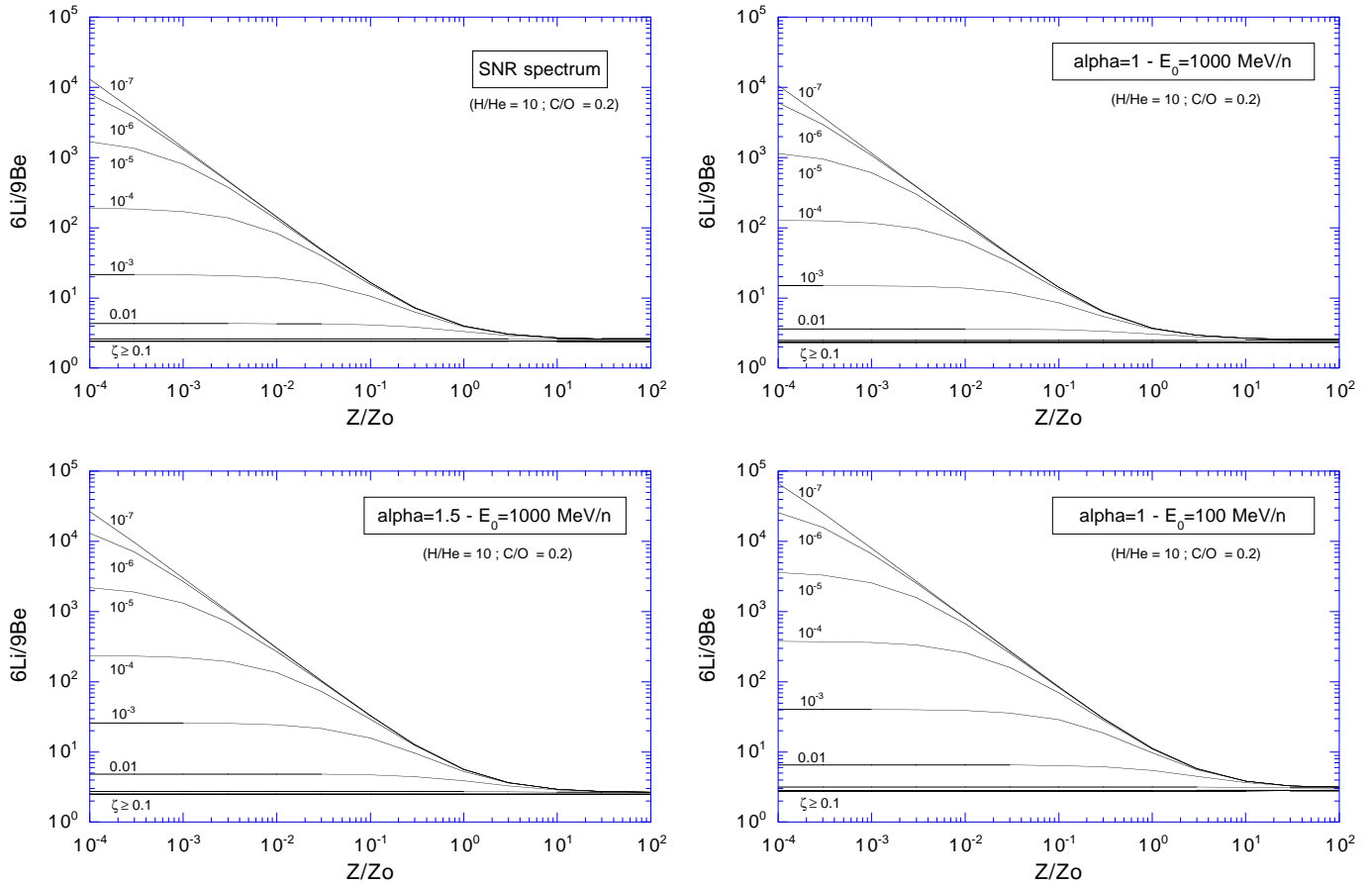


**Fig. 4.** Production ratio of  ${}^6\text{Li}$  and  ${}^9\text{Be}$  by spallation, for different EP spectra and compositions, and different target compositions, as in Fig. 3.

and Fields & Olive (1999) proposed different models to account for the decrease of  ${}^6\text{Li}/{}^9\text{Be}$  with metallicity. In any case, however, the above qualitative and quantitative analysis based on steady-state calculations show that the SB model is a very good candidate to solve the LiBeB evolution problem in the early Galaxy, by naturally predicting an EP composition having the appropriate reduced metallicity to provide both the correct Be production efficiency and the correct  ${}^6\text{Li}/{}^9\text{Be}$  ratio. We now show that this model indeed works when applied more accurately using time-dependent calculations.

### 3.2. Time-dependent calculations for the SB model

The SB model has been described above in Sect. 2. The main parameters are the mechanical power,  $\mathcal{P}_{\text{in}}$ , provided by the OB association to the superbubble ( $\mathcal{P}_{\text{in}} = 10^{38}$  erg for all the plots shown here), the lifetime of the SB,  $\tau_{\text{SB}}$ , the ambient ISM density,  $n_0$ , the SN explosion model (UA or TA, from WW95), the EP spectrum (SNR or SB spectrum, with index  $\alpha = 1$  or 1.5), and the cut-off energy,  $E_0$ , of the spectrum (except for the SNR spectrum, where it is assumed constant at  $10^{14}$  eV/n).

In Fig. 5, we show the detailed Be production rate as a function of time for a SB spectrum with  $\alpha = 1$  and  $E_0 = 300$  MeV/n, and an ISM density of  $1 \text{ cm}^{-3}$ . As expected, the main producing reaction is the spallation of  ${}^{16}\text{O}$  by the H nuclei, because O is

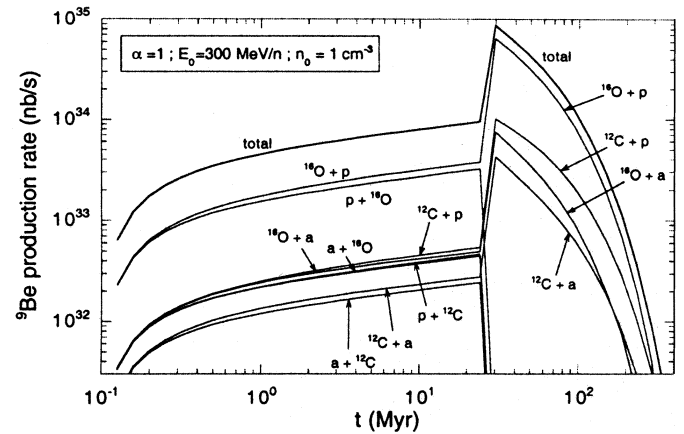


**Fig. 5.** Detailed Be production rate by the SB model, as a function of time. The EP spectrum is a SB spectrum with spectral index  $\alpha = 1$  and a cut-off energy of  $E_0 = 300$  MeV/n, as indicated. The ambient ISM density is  $1 \text{ cm}^{-3}$ . The labels of the curves refer to the corresponding spallation reaction, where the first nucleus mentioned is the energetic one.

the most abundant metal in the SN ejecta. The total production rate is shown to increase during the whole lifetime of the SB (here  $\tau_{\text{SB}} = 30$  Myr), as a result of the following competing effects: i) the accumulation of the EPs in the SB, ii) the decrease

of the EP and target metallicity ( $\propto t^{-6/35}$ ), iii) the Coulombian energy loss of the EPs, and the rarefaction of the gas inside the expanding SB. Neglecting the energy losses (which act on a longer timescale, because of the low SB density), it is easy to estimate the time dependence of the Be production rate:

$$\frac{d\mathcal{N}_{\text{Be}}}{dt} \propto \mathcal{N}_{\text{EP}} \alpha_{\text{O}} n_{\text{SB}}, \quad (9)$$

where  $\mathcal{N}_{\text{EP}}$  is the total number of EPs in the SB and  $\alpha_{\text{O}}$  is the fraction of Oxygen in the EPs (inverse spallation) or the SB gas (direct spallation).

Now  $\mathcal{N}_{\text{EP}} \propto t$ , because the acceleration rate is constant, and  $\alpha_{\text{O}} \propto t^{-6/35}$ , as already mentioned. Considering the time dependence of  $n_{\text{SB}}$  (Eq. 3), we thus obtain  $d\mathcal{N}_{\text{Be}}/dt \propto t^{1/5}$ , in very good agreement with the  $d\mathcal{N}_{\text{Be}}/dt \propto t^{0.22}$  obtained from Fig. 9 by a fit between 1 and 10 Myr. Note finally that, at a given time, the fraction of Oxygen,  $\alpha_{\text{O}}$  is actually slightly higher in the EPs than in the SB, because the EPs collect particles accelerated at earlier times when the metallicity was higher, which explains why the inverse spallation reaction  ${}^{16}\text{O} + p$  actually dominates, as seen on Fig. 5.

As expected, Fig. 5 also shows the (discontinuous) increase of the production rates at  $\tau_{\text{SB}}$ , when the EPs leave the SB and interact with a much denser medium. The situation has been idealized here, as we should not expect that the EPs leave the SB instantaneously at  $\tau_{\text{SB}}$ , nor that they be ‘perfectly confined’ within the SB before  $\tau_{\text{SB}}$ . However, as we emphasized above, this idealized scenario does provide the correct *total* Be yield, while giving a valuable insight on the respective role of direct and inverse spallation reactions. For example, it is evident that only the latter are efficient in the low metallicity target relevant at  $t > \tau_{\text{SB}}$ . The nuclear reaction rates are also seen to decrease after  $\tau_{\text{SB}}$ , due to the Coulombian energy losses in the higher density medium. As mentioned at the end of Sect. 2.3, we arbitrarily chose the target density to be  $0.1 \text{ cm}^{-3}$  after  $\tau_{\text{SB}}$ . This choice has no influence on the total Be yield, since once the acceleration has stopped, the integral of the reaction rates is independent of density (see Parizot & Drury, 1999a, for more details).

This is no longer true, however, when the dynamics of the SB evolution is involved (Parizot & Lehoucq 1999). This is shown on Fig. 6, where the Be production rate is plot as a function of time, for different values of the ambient density. For  $t < \tau_{\text{SB}}$ , the reaction rates are proportional to the SB density, that is to  $n_0^{19/35}$ , while after  $\tau_{\text{SB}}$ , the EPs lose energy on a time scale all the shorter that the density is high. Concerning the total, integrated yields of Be, they are also indicated on Fig. 6. They show only a weak dependence on the ambient density, which results from the fact that most of the Be nuclei are produced by EP interactions outside the SB, or in the dense shell of interstellar gas. Note that we have used here a different prescription for the target density after  $\tau_{\text{SB}}$ . It has been chosen so as to ensure the continuity of the production rates.

The same has been used in Fig. 7, where we show the Be production rate as a function of time for a SB spectrum with index  $\alpha = 1.5$ , for different values of the cut-off energy. We

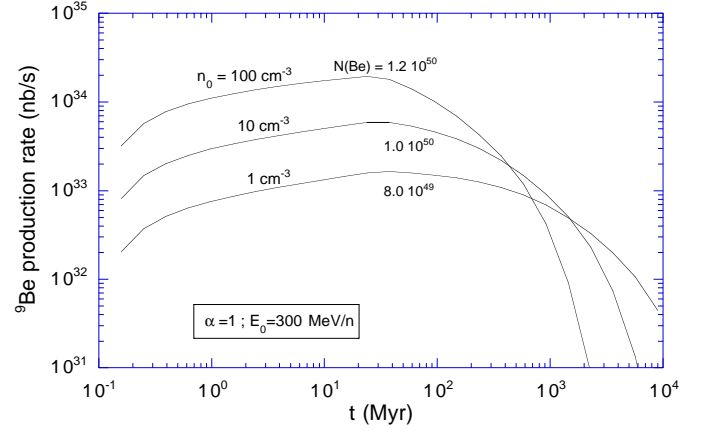


**Fig. 6.** Be production rate (in number of nuclei per second) as a function of time for the same SB model as in Fig. 9, but for different ISM densities. The total, integrated Be yield is indicated in each case, beside the corresponding curve.

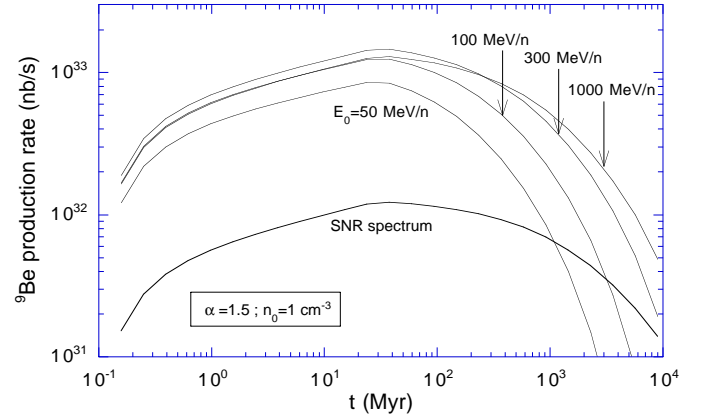


**Fig. 7.** Be production rate as a function of time, for SB models using the SB spectrum with index  $\alpha = 1.5$  and different cut-off energies. The case of a SNR source spectrum is also shown.

also show, for the sake of comparison, the Be production rate obtained with the SNR spectrum. It is clearly less efficient, as expected from the steady-state analysis above, although the production rates decrease less quickly after  $\tau_{\text{SB}}$ , because of the high energy particles, which keep supernuclear energies (i.e. above nuclear reaction thresholds) for a longer time.

The most important results relate to the total Be yield,  $\mathcal{N}_{\text{Be}}$ , obtained with the SB model. This is obtained by merely integrating the production rates over time. The results are shown on Fig. 8, for different spectra, as a function of the cut-off energy,  $E_0$ . The horizontal dashed line corresponds to the observed value of the Be/O ratio, derived as explained above (in this model, the SB is blown by 100 SNe, which must be accompanied by the production of  $\sim 6 \cdot 10^{49}$  of Be). As can be seen, the results of our SB model are in very good agreement with the observations, if the EP spectrum is of the SB type, with a cut-off energy of a few hundreds of MeV/n. Interestingly enough, this is just the energy range predicted by the SB acceleration model (Bykov & Fleishman, 1992; Bykov, 1995,1999). On the other

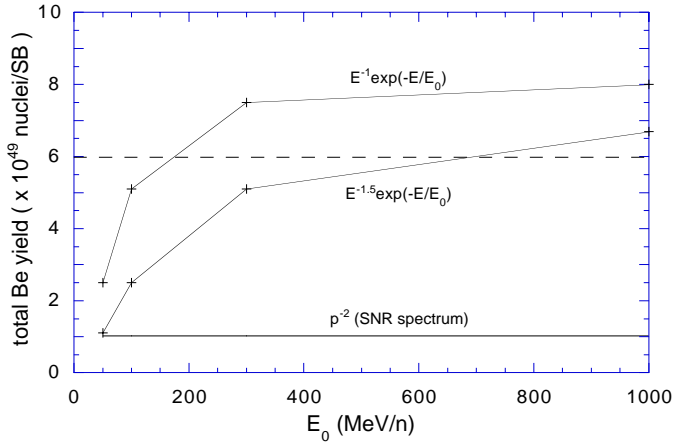


**Fig. 8.** Total Be yields of the SB for different EP spectra, as a function of the cut-off energy,  $E_0$ . For the SNR spectrum, the cut-off energy is irrelevant, and we show a constant yield. The dashed line corresponds to the yield required to explain the observed Be/O ratio (see text). In this SB model, a total of 100 SNe have exploded during the SB lifetime of 30 Myr.

hand, the standard SNR spectrum leads to a Be yield a factor of 6 too low, which rules out this spectrum unless strongly selective acceleration is invoked.

An enhancement of the C and O abundance relative to H and He by a factor of 6 does not seem unrealistic at first glance. Indeed, the study of the CR composition indicates that a similar enhancement by a factor of  $\sim 8$  must have occurred if the cosmic rays are accelerated out of the ISM. Moreover, such an enhancement is satisfactorily accounted for by the theoretical CR acceleration model of Ellison et al. (1997), where refractory elements are locked in grains and preferentially accelerated, while the acceleration of volatile elements (like H and He) is less efficient. However, the selectivity of this acceleration mechanism depends to a large extent on the physical conditions in the ambient medium, notably the temperature, which determines the degree of ionization of the different nuclei, and the fraction of the elements which are locked into grains. Therefore, it is not clear whether the specific conditions prevailing in a SB give rise to the same enhancement of C and O as in the usual ISM. Additional work would thus be needed to determine whether a selective acceleration mechanism increasing  $\zeta_{EP}$  by a factor of 6 in the SB is reasonable or not.

As it stands, two opposite positions can be adopted within the framework of the SB model: i) holding on to the SB acceleration mechanism of Bykov et al. and thus to the SB spectrum, because it does not require any selective acceleration, or ii) preferring to invoke selective acceleration and keep the usual SNR (cosmic ray source) spectrum, because it does not require a different acceleration mechanism. Both points of view seem to be acceptable in the current state of knowledge, and provide genuine solutions to the LiBeB evolution problem in the early Galaxy, as we have shown. Additional theoretical work, relating to the SB acceleration mechanism on the one hand, and to the selectivity of the CR acceleration mechanism under the physical

conditions prevailing in a SB, on the other hand, is now needed to decide between these two stances.

Interestingly enough, a full solution of the  ${}^6\text{LiBeB}$  problem therefore appears to be able to provide important information about related fields in high energy astrophysics. For instance, one important remaining questioning about energetic particles in the Galaxy concerns the part of the spectrum below 1 GeV/n. Since these so-called low energy cosmic rays are prevented from reaching the inner solar system by the magnetic fields associated with the solar wind, we cannot get any direct information about their spectrum and composition. While it may seem reasonable to assume that these are similar to the ordinary cosmic rays (CRs), it remains perfectly possible that a second component of EPs, with different origin, spectrum and composition, also exists at low energy ( $E \lesssim 1$  GeV/n) and is superimposed to the ordinary CRs. Now since virtually all the spallative LiBeB nuclei are expected to be produced by these low energy cosmic rays, whatever their spectrum and composition, it is clear that strong constraints on their characteristics should come out of a detailed study of the light element evolution in the Galaxy. The results presented here seem to indicate that the SBs could well be the source of an important component of EPs, dominating the usual CRs at low energy, and therefore being responsible for most of the LiBeB production in the Galaxy.

#### 4. Conclusion

In this paper we have shown that, even in the very early Galaxy, superbubbles are natural sources of C and O-rich energetic particles with a metallicity of about  $10^{-1}Z_{\odot}$ , even within the most conservative assumption concerning the mixing and dilution of the SN material ejected inside the SB with the ISM gas evaporated of the expanding SB shell and/or embedded clouds. We further showed that these enriched EPs have enough energy to produce as much Li, B and Be as observed in the metal-poor halo stars. This SB model thus provides a solution of the long-standing problem of LiBeB evolution in the early Galaxy. In addition, it offers a straightforward way to account for the most recent  ${}^6\text{Li}$  data at low metallicity, as discussed in Sect. 3.1.

From our point of view, the most tantalizing solution seems to be the SB model using the so-called SB spectrum, as derived from the SB acceleration model of Bykov et al., since it does not require any ad hoc assumption concerning the mixing of the SN ejecta and the chemical selectivity of the acceleration mechanism. However, from another point of view, it could be argued that invoking a selective acceleration and/or a very imperfect mixing of the gas inside the SB is preferable, because it avoids the recourse to an energy spectrum different from the cosmic rays.

One of the main original features of our model is that it implies a decoupling between the metallicity of the stars and their age, or in other words, a non monotonic Galactic enrichment. In particular, stars formed at the same time can have metallicities spreading over two orders of magnitude or more. Indeed, as discussed in Sect. 2.1, a SB developing in the early Galaxy within an medium of metallicity, say,  $10^{-4}Z_{\odot}$ , provides  $\lesssim 10^5 M_{\odot}$

of gas enriched to  $\sim 10^{-1}Z_{\odot}$ , with the observed Be/O and LiBeB abundance ratios. This gas then mixes with the ambient low-metallicity gas and collapses to form stars of various metallicities, ranging from, say,  $10^{-4}$  to  $10^{-1}Z_{\odot}$ . Evidently, all these stars show the same abundance ratios, and the linear increase of the Be and B abundances with the stellar metallicity is, in this model, the manifestation of a *dilution line*. As all the SBs are expected to behave in much the same way, the Be/Fe ratio, for instance, obtained at the end of any SB lifetime should also be approximately the same, and all the individual dilution lines overlap to give a general apparent linear growth of Be/Fe as a function of Fe/H, as seen from the observational data.

Interestingly enough, this special feature of the SB model can be tested observationally. Indeed, if the distribution of halo stars over the metallicity range  $10^{-4}$ – $10^{-1}Z_{\odot}$  is the result of dilution lines, then the same number of stars should be expected at all  $Z$ . This is in contrast with the expectations of a scenario in which Be, B, O and Fe abundances build up continuously and monotonically in the Galaxy. Indeed, in such a model, more stars should be expected at low metallicity, because their formation would correspond to a time when the star formation rate was higher (more gas in the Galaxy). In fact, the SB model even predicts an increasing number of stars at increasing metallicity, because the new generation of stars (at the end of the SB lifetime) should be distributed from  $Z_{\text{ISM}}$  to  $Z_{\text{SB}} \sim 10^{-1}Z_{\odot}$ , and  $Z_{\text{ISM}}$  irremediably increases. Of course, a strong observational bias may make this prediction rather hard to test, as it is easier to measure very small abundances at higher metallicity. However, a more systematic observational work with increased numbers of stars (and thus improved statistics) may lead to a definite test of the SB model in the future.

Our model also allows one to evaluate the expected dispersion of the stars in the data. Varying the SB parameters, we were able to obtain a range of Be/O ratios as the final output of the model, all of them laying in the observationally allowed numbers. We first investigated OB associations containing less than 100 SNe (our standard value). There are two different ways to do so: i) keeping a SN explosion rate of one every  $3 \cdot 10^5$  yr, but shortening the SB lifetime, or ii) keeping a SB lifetime of 30 Myr, but lowering the explosion rate and thus the SB mechanical power and the power imparted to the EPs. We explored the first possibility down to lifetimes of 10 Myr, and found an increase of the Be/O and Be/Fe ratios by about 20%. This is mostly due to a correspondingly higher reduced metallicity of the EPs (see Fig. 1). As for the second possibility, we investigated mechanical powers down to  $10^{37} \text{erg s}^{-1}$  (i.e. one SN every 3 Myr) and found Be/O and Be/Fe ratios about 40% lower, in agreement with the results shown in Fig. 1.

Another cause for the dispersion of the data is expected from the overlap of dilution lines corresponding to SBs evolving in an interstellar medium of different metallicity. We run the model for an ambient metallicity of  $10^{-2}Z_{\odot}$ , using the corresponding SN models of WW95 (models TA), and found Be/O and Be/Fe ratios about 40% higher than for a metallicity of  $10^{-4}Z_{\odot}$ . Gathering all these results, we finally expect a dispersion of about a factor of 2 or 3 in the data, corresponding to stars formed

from the gas processed by SBs created by OB associations with different characteristics.

Note also that, in our calculations, we have used an idealized SB model. However, the results should not be very different for a real SB, as far as LiBeB production is concerned. In particular, the time history of the energy release in the OB association is not very important, as a given amount of energy imparted to EPs with a given composition, always leads to approximately the same integrated LiBeB production, independently of the rate at which the energy is injected. As for the EP composition, it mainly depends on the amount of material evaporated off the shell, as compared with the total mass of the ejecta. But both are directly linked to the number of SNe exploding within the SB, and do not depend (or little) on the rate of explosions. To put it in different words, no matter what the exact explosion rate is, one should always be able to define a modified time coordinate ('renormalized' time),  $t'$ , such that  $\mathcal{P}' \equiv dE_{\text{SN}}/dt'$  is constant and the SB evolution laws Eq. (1)–(4) approximately hold with this new time coordinate. Our calculations of the LiBeB production would thus give results very close to those obtained in the genuinely continuous model.

Finally, we argue that apart from the intrinsic dispersion in the data discussed above, one should also find in the halo some stars formed from a part of the ISM which has not been processed by SBs. This set of stars is expected to show a very different behavior, since it results from the activity of individual, isolated SNe, rather than collective ones, in an OB association. Some LiBeB production should nevertheless accompany the SN energy release, but it now occurs within supernova remnants (SNRs), not superbubbles. Now the LiBeB production within isolated SNRs has been calculated in detail in precedent papers (Parizot & Drury, 1999a,b), and shown to lead to Be/O and Be/Fe ratios much lower (by about one order of magnitude) than those obtained in the SB model presented here. These isolated SNe, however, and the accompanying LiBeB production process, have no reason not to occur, and should be responsible for the general, continuous increase of the ISM metallicity. But the stars formed from this gas should be expected to lay on a specific part of the diagram showing, say, the Be abundance as a function of Fe/H, namely on a line about one order of magnitude lower than the line corresponding to the stars formed from the SB processed gas. This is another prediction of the model (unless *all* the SNe occurred in OB associations in the early Galaxy, which is not very likely). Unfortunately, the B and Be abundance is obviously very hard to measure in these stars, since it is expected to be so low. Most probably, observations will provide upper limits on these abundances. In this respect, it is very interesting to note that only upper limits have been reported for 7 stars in the sample gathered by Fields & Olive (1999). Although more observational work and proper statistics would be needed, these stars might represent a first piece of evidence in favour of a 'bimodal' LiBeB production in the Galaxy, that is to say from *correlated* and *isolated* SN explosions.

*Acknowledgements.* We wish to thank Andrei Bykov and Jean-Paul Meyer for comments improving the content as well as the presentation

of the paper. This work was supported by the TMR programme of the European Union under contract FMRX-CT98-0168.

## References

- Anders E., Grevesse N., 1989, *Geochim. Cosm. Acta* 53, 197
- Boesgaard A.M., King J.R., Deliyannis C.P., Vogt S.S., 1998, in press
- Bomans D.J., Chu Y.-H., Hopp U., 1997, *AJ* 113, 1678
- Brown A.G.A., de Geus E.J., de Zeeuw P.T., 1995, *A&A* 289, 101
- Bykov A.M., 1995, *Space Sci. Rev.* 74, 397
- Bykov A.M., 1999, In: Ramaty R., Vangioni-Flam E., Casse M., Olive K. (eds.) *LiBeB, cosmic rays and gamma-ray line astronomy*. ASP Conference Series
- Bykov A.M., Fleishman G.D., 1992, *MNRAS* 255, 269
- Cassé M., Lehoucq R., Vangioni-Flam E., 1995, *Nat* 374, 337
- Cayrel R., Spite M., Spite F., et al., 1999, *A&A*, in press (astro-ph/9901205)
- Cioffi D.F., Shull J.M., 1991, *ApJ* 367, 96
- Ellison D., Drury L.O'C., Meyer J.-P., 1997, *ApJ* 487, 197
- Fields B.D., Olive K.A., 1999, *ApJ*, in press (astro-ph/9811183)
- Higdon J.C., Lingenfelter R.E., Ramaty R., 1998, *ApJ* 509, L33
- Hobbs L.M., Thorburn J.A., 1994, *ApJ* 428, L25
- Hobbs L.M., Thorburn J.A., 1997, *ApJ* 491, 772
- Israeli G., García-López R.J., Rebolo R., 1998, *ApJ* 507, 805
- Mac Low M.M., McCray R., 1988, *ApJ* 324, 776
- Meneguzzi M., Audouze J., Reeves H., 1971, *A&A* 15, 337
- Parizot E., Drury L., 1999a, *A&A* 346, 329
- Parizot E., Drury L., 1999b, *A&A* 346, 686
- Parizot E., Drury L., 1999c, In: Ramaty R., Vangioni-Flam E., Casse M., Olive K. (eds.) *LiBeB, cosmic rays and gamma-ray line astronomy*. ASP Conference Series
- Parizot E., Lehoucq R., 1999, *A&A* 346, 211
- Ramaty R., Lingenfelter R.E., 1999, In: Ramaty R., Vangioni-Flam E., Casse M., Olive K. (eds.) *LiBeB, cosmic rays and gamma-ray line astronomy*. ASP Conference Series
- Ramaty R., Kozlovsky B., Lingenfelter R.E., 1996, *ApJ* 456, 525
- Ramaty R., Kozlovsky B., Lingenfelter R.E., Reeves H., 1997, *ApJ* 488, 730
- Reeves H., Fowler W.A., Hoyle F., 1970, *Nat* 226, 727
- Shull J.M., Saken J.M., 1995, *ApJ* 444, 663
- Smith V.V., Lambert D.L., Nissen P.E., 1998, *ApJ* 506, 405
- Tomisaka K., 1992, *PASJ* 44, 177
- Vangioni-Flam E., Cassé M., 1999, In: Spite M., Crifo F. (eds.) *Galaxy Evolution: connecting the distant universe with the local fossil record*. Les Rencontres de l'Observatoire de Paris, Kluwer, Dordrecht, in press
- Vangioni-Flam E., Ramaty R., Olive K.A., Cassé M., 1998, *A&A* 337, 714
- Vangioni-Flam E., Cassé M., Cayrel R., et al., 1999, *New Astronomy*, in press (astro-ph/9811327)
- Walter F., Kerp J., Duric N., Brinks E., Klein U., 1998, *ApJ* 502, L143
- Weaver R., McCray R., Castor J., Shapiro P., Moore R., 1977, *ApJ* 218, 377
- Woolsey S.E., Weaver T.A., 1995, *ApJS* 101, 181
- Zanin C., Weinberger R., 1997, *A&A* 324, 1165